

# A TWO-DIMENSIONAL DYNAMIC PARTICLE MODEL OF THE SURFACE CCD TRANSPORT PROCESS

W Fawcett\* and G F Vanstone\*

## ABSTRACT

The transport of minority carriers in a surface CCD is investigated using a particle model which takes full account, under dynamic conditions, of the influence on the surface potential of both the minority carriers and the two-dimensionality of the depletion region.

## INTRODUCTION

In a surface CCD, the motion of the minority carriers carrying the signal charge is determined by the electrostatic potential distribution near the semiconductor-oxide interface. This potential distribution is controlled externally through the voltages applied to the device electrodes, but since both the minority and majority carriers distribute themselves according to the electric fields within the semiconductor, the precise form of the potential distribution must take this into account and be determined self-consistently. In addition, since the carrier redistribution takes a finite time, even for fixed contact potentials, a study of the transport processes must in general allow for a time-dependent potential distribution.

In order to determine the potential distribution, a number of models have been developed previously. However, in general, these have been static approaches, in that it has been assumed that the majority carriers instantaneously distribute themselves according to the applied potentials, and the effect of the minority carriers has been neglected. In addition, the distribution of majority carriers has usually been determined by the one-dimensional depletion approximation.

In this paper we present some preliminary results of a microscopic computer simulation of CCD operation which is restricted by none of these approximations. Thus the limit of the depletion region, as defined by the distribution of the majority carriers, is determined dynamically in two-dimensions, and the effect of the signal charge under both static and dynamic conditions is fully taken into account.

\* Royal Radar Establishment, St Andrews Road, Malvern, Worcs., ENGLAND

## DESCRIPTION OF THE MODEL

The principle of the computational technique is based on the particle model described by Hockney (ref. 1) in connection with plasma simulations. This technique as applied to semiconductor device analysis has been discussed recently by Hockney and Reiser (ref. 2). The essential steps in the calculation are:-

- (1) The majority and minority carriers are represented by a large number of particles and the spatial coordinates of each of the particles are assigned values according to the initial conditions. Usually the majority carriers would be distributed throughout the device, while the minority carriers would be injected below the appropriate device electrode.
- (2) The charge density within the device is specified on a square mesh and determined by assigning the particles with appropriate weights to the neighbouring mesh points.
- (3) The potential distribution is calculated by numerical solution of the two-dimensional Poisson equation. Since the usual CCD structure is periodic in the direction of the charge transfer, the method developed by Hockney (ref. 3) based on Fourier transform techniques and using recursive cyclic reduction was found to be very suitable. This technique was generalised to incorporate an oxide layer on the semiconductor surface along with the necessary boundary conditions at the oxide-semiconductor interface.
- (4) The electric field acting on each of the particles is calculated using the potential distribution determined in step (3), and the position of each particle advanced during a small time step according to the carrier mobility and electric field. Diffusion is included by adding a random walk with a root mean square displacement determined by the diffusion coefficient.
- (5) Steps (2) to (4) are repeated for many time steps.

Certain criteria need to be satisfied for this procedure to produce satisfactory results. Firstly, the number of particles must be chosen large enough to obtain a low statistical fluctuation. For this purpose it was found that using 5000 particles to represent the majority carriers and 500 for the minority carriers was more than adequate. Secondly, the mesh spacing must be made small enough to produce the necessary resolution which in practice means the mesh spacing must be of order or less than the Debye length. The technique used to solve Poisson's equation requires the number of points in the periodic direction parallel to the semiconductor-oxide interface to be  $2^p$ , where  $p$  is integral, and it was then found that 64 or 128 points proved suitable for most device geometries. Perpendicular to the interface, the technique requires the number of mesh points in the semiconductor to be  $2^q + 2$ , where  $q$  is integral, and typically 18 or 34 points were used. The same requirement applies to the oxide layer but here only 6 or 10 points proved necessary. The time step must be chosen small enough to justify the assumption that the electric field does not change significantly during the particle trajectory. Since the mesh spacing needs to be chosen to adequately represent the electric field variations, this means in practice that the time step must be small enough for the

particle to move a distance less than this mesh spacing. Essentially this requirement means that the time step must be limited to a fraction of the dielectric relaxation time which in p-type silicon with a doping density of  $5 \times 10^{20} \text{ m}^{-3}$  is about  $2 \times 10^{-11} \text{ s}$ .

### RESULTS

We present in this section some of the preliminary results obtained with the particle model described in the previous section. The object of these calculations was to investigate the charge redistribution and changes in the surface potential which occur during the early stages of the transfer of signal charge between adjacent electrodes. A simple 3-phase narrow-gap surface channel device was modelled as shown in figure 1. All the results described below were obtained using an electrode width of  $1.2 \times 10^{-5} \text{ m}$ , an electrode gap of  $3 \times 10^{-6} \text{ m}$ , an oxide thickness of  $3 \times 10^{-7} \text{ m}$  and a p-type silicon substrate with a doping density of  $5 \times 10^{20} \text{ m}^{-3}$ . A fixed positive charge density at the oxide-silicon interface was incorporated in all the calculations and assigned a value of  $10^{15} \text{ m}^{-2}$ .

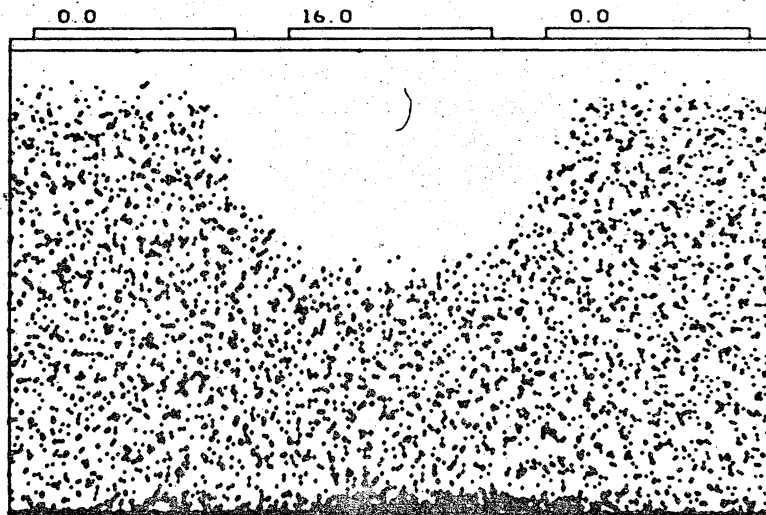


FIGURE 1 Distribution of majority carriers calculated  $6 \times 10^{-10} \text{ s}$  after the application of 16V to electrode 2.

Figure 1 shows the spatial distribution of majority carriers calculated  $6 \times 10^{-10} \text{ s}$  after the application of 16V to electrode 2. No minority carriers were incorporated in this calculation. The curved, almost semicircular, shape of the depletion edge with some penetration under electrodes 1 and 3 is clearly seen. Depletion regions also exist under electrodes 1 and 3 because of the fixed positive interface charge. It was found that the depletion layer under electrode 2 formed in initially neutral material in a time of order  $5 \times 10^{-11} \text{ s}$  although those under electrodes 1 and 3 could take an order of magnitude longer to form due to the much lower fields at the surface of these regions.

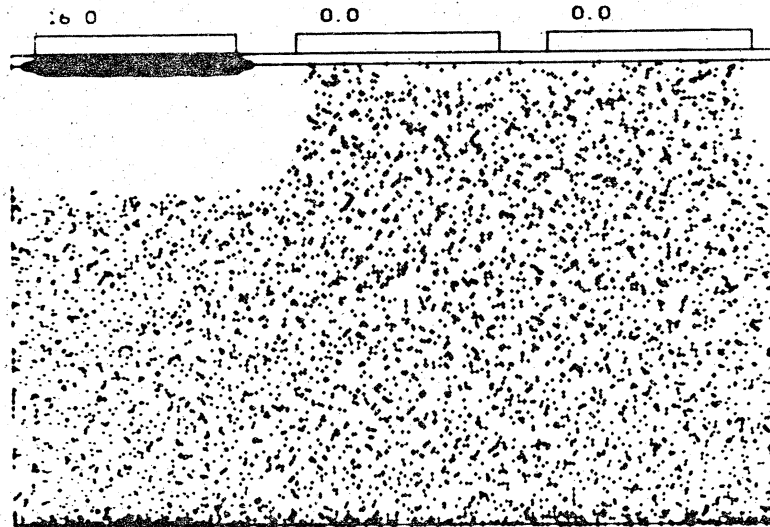


FIGURE 2 Distribution of majority carriers calculated  $10^{-10}$  s after the application of 16V to electrode 1 with a minority carrier density of  $6 \times 10^{15} \text{ m}^{-2}$  distributed along the interface below the electrode. (The apparent spread of the minority carriers perpendicular to the interface is due to unavoidable photographic over exposure).

Figure 2 shows the same device after a time of  $10^{-10}$  s with the potential now applied to electrode 1 and with a minority carrier density of  $6 \times 10^{15} \text{ m}^{-2}$  injected below this electrode. In this case, the depletion edge is much flatter beneath the electrode due to the presence of the minority carriers. The inability of the depletion layer to form under electrodes 2 and 3 on this time scale is evident.

Starting with the situation in figure 2, the potential on electrode 1 was decreased linearly to zero volts in a time of  $2 \times 10^{-11}$  s while over the same period the voltage on electrode 2 was increased to 16V. The particle distribution which resulted at a time of  $4 \times 10^{-10}$  s, i.e.  $3 \times 10^{-10}$  s after the start of the voltage switch, is shown in figure 3. As expected, the dominant feature is the transfer of the depletion region and some of the minority carriers from below electrode 1 to below electrode 2. In addition, however, it is noted that of those minority carriers remaining under electrode 1, some have moved a significant distance into the silicon substrate, while others have transferred to below electrode 3. This implies, because of the assumed periodicity of the structure, that minority carriers have transferred in both directions from electrode 1 rather than only to electrode 2 as is expected and required.

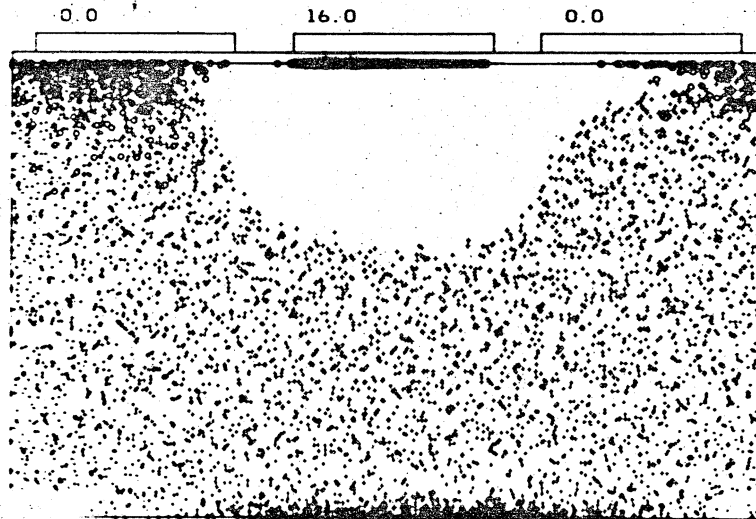


FIGURE 3 Distribution of majority and minority carriers  $3 \times 10^{-10}$  s after the voltage is switched to electrode 2 from the situation shown in figure 2. The minority carriers are represented by circles.

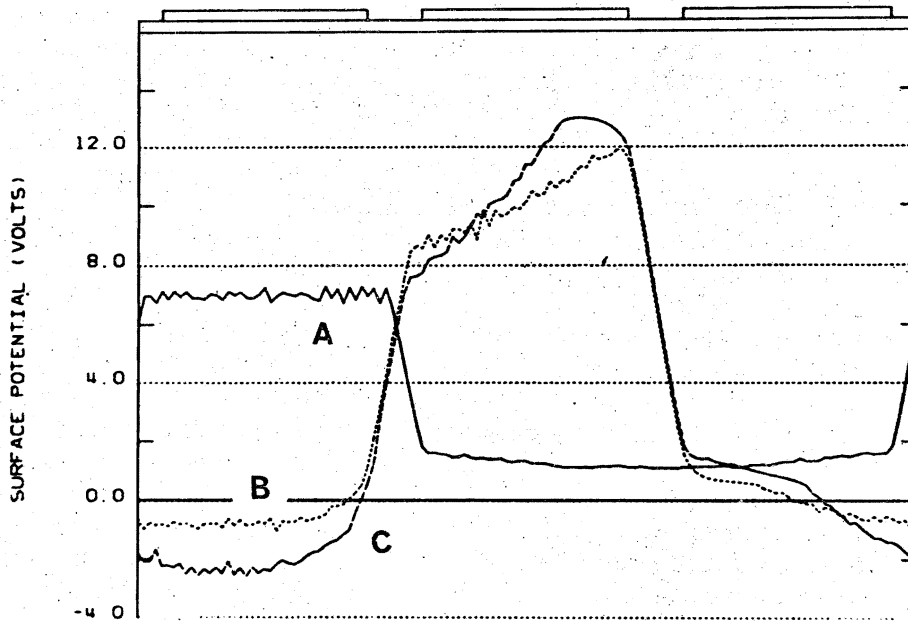


FIGURE 4 Variation of the potential along the semiconductor-oxide interface at times of (A)  $10^{-10}$  s, (B)  $3 \times 10^{-10}$  s and (C)  $2 \times 10^{-10}$  s.

These features can be explained by reference to figure 4 which shows the surface potential at the oxide-semiconductor interface at times of  $10^{-10}$ s i.e. just before the voltages are switched (curve A),  $2 \times 10^{-10}$ s (curve C) and  $3 \times 10^{-10}$ s (curve B). It is immediately evident from curve C that after the voltages are switched and the potential on electrode 1 returns to zero, the surface potential under this electrode goes negative due to the presence of the minority carriers. This explains the movement of minority carriers into the silicon substrate under this electrode. The negative surface potential also explains the transfer of minority carriers to electrode 3 because the surface potential under this electrode is of course positive. As the minority carriers move away from electrode 1, the surface potential in this region becomes more positive but nevertheless will remain negative so long as sufficient minority carriers exist in this region. It is noted that if the minority carrier density does not exceed the fixed positive interface charge density, a negative surface potential would not be expected. In this case the minority carriers would not be expected to move away from the surface although the transfer to electrode 3 would still occur. Charge movements of this type have also been suggested by M P Singh et al (ref. 4).

The effect on the surface potential of the transfer of minority carriers from electrode 1 to electrode 2 is also shown in figure 4. Immediately the voltage is switched to electrode 2, those minority carriers nearest electrode 2 are swept by the high electric field across the inter-electrode gap. The low electric field under contact 2 however, means that the carriers slow down on reaching the edge of the contact producing bunching in this region. The effect of this bunching is to reduce the surface potential under the edge of electrode 2 and thus produce an electric field across the region under the electrode. These features are clearly demonstrated in curve C of figure 4. After this initial stage, the flow of minority carriers tends to slow down, partly because of the depression of the surface potential under electrode 2, but also because the minority carriers now require to traverse the low-field region under electrode 1. The minority carriers under electrode 2 gradually distribute themselves across the region under the electrode and it is found that after about  $6 \times 10^{-10}$ s the surface potential is nearly uniform in this region.

The transfer of minority carriers to electrode 3 and their drift into the bulk of the semiconductor can be eliminated by reducing the voltage on electrode 1 to some finite positive value rather than to zero.

In this way the surface potential under electrode 1 can be maintained positive and greater than that under electrode 3. The precise value of the voltage to be maintained on electrode 1 will clearly be larger for larger minority carrier densities. Calculations have been carried out for minority carrier densities of  $10^{15}$ ,  $3 \times 10^{15}$  and  $6 \times 10^{15} \text{ m}^{-2}$  of the efficiency of the transfer process during the initial stages of transfer when electrode 1 is returned to 5V rather than zero. All the other parameters were as described above. The results are shown in figure 5. In all three cases, it was found that minority carriers remained close to the surface and transferred to electrode 2. As shown in figure 5 the transfer inefficiency at short times becomes less as the minority density increases. This would seem to result primarily from the depression of the surface potential by the minority carriers enhancing the electric field between the electrodes.

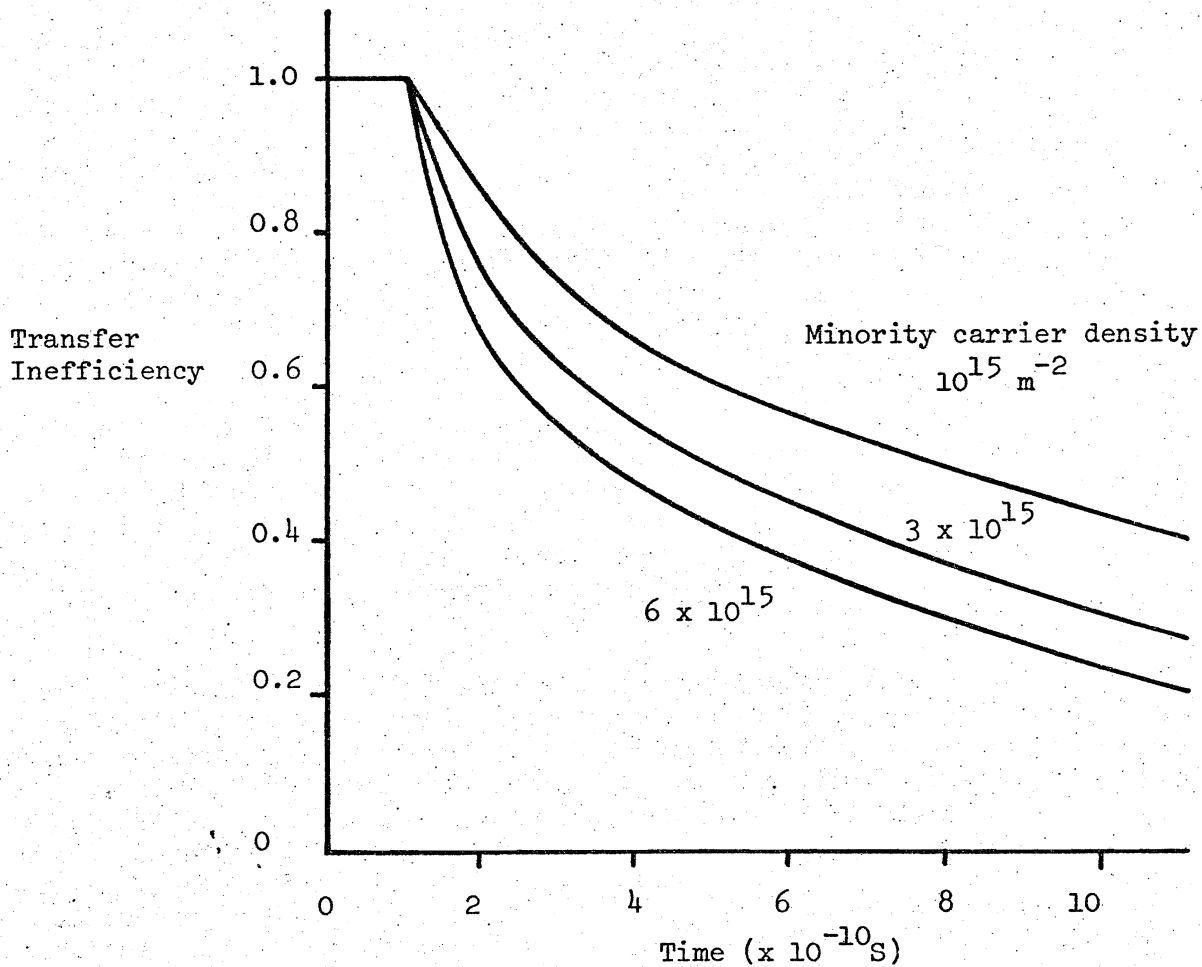


FIGURE 5 Variation of transfer inefficiency with minority carrier density.

#### ACKNOWLEDGEMENTS

We are extremely grateful to Dr D P Jenkins for writing the computer subroutine to solve Poisson's equation.

This paper is contributed by permission of the Director RRE, Copyright Controller HMSO.

#### REFERENCES

- 1 R W Hockney, Phys Fluids 9, 1826 (1966)
- 2 R W Hockney and M Reiser, IBM Res Rpt RZ 482 (Zurich, Switzerland) Feb 1972
- 3 R W Hockney, J Ass Comp Mach 12, 95 (1965)
- 4 M P Singh and S D Brotherton, private communication